Reducing Circulating Currents in Interleaved Converter Legs under Selective Harmonic Elimination Pulse-width Modulation

Georgios Konstantinou[(1)], Josep Pou[(1),(2)] Gabriel J. Capella[(2)], Salvador Ceballos[(3)] and Vassilios G. Agelidis[(1)]
[(1)] UNSW Australia, Sydney, NSW, 2052, Australia
[(2)] Technical University of Catalonia, Catalonia, Spain [(3)] Tecnalia Energy, Spain
email: g.konstantinou@unsw.edu.au, j.pou@unsw.edu.au, gabriel.jose.capella@upc.edu,
salvador.ceballos@tecnalia.com, vassilios.agelidis@unsw.edu.au

***Abstract*—Interleaving of voltage source converter legs enables higher output currents per phase, effectively increasing the power rating without increasing semiconductor ratings. Different switching patterns between the converter legs increase the number of Thevenin output voltage levels and, hence, the quality of the waveform but also generate circulating currents within one phase. This paper proposes a controller for interleaved converter legs under selective harmonic elimination pulse-width modulation (SHE-PWM) aimed at reducing the circulating current within the legs of each phase. The controller is used in combination with optimally selected SHE-PWM patterns to minimise the peak value of the circulating current. The proposed controller is applied in two interleaved three-level active neutral-point-clamped converters and simulation results demonstrate their performance.**

***Index Terms*—Interleaving, multilevel converters, multilevel waveforms, parallel legs, selective harmonic elimination, SHE-PWM, voltage source converters,**

I. Introduction

Interleaving of voltage source converter (VSC) legs provides an effective way of increasing the power rating of a power converter without the need for parallel connection of semiconductor devices [1]–[7] applicable to both two-level and multilevel converters [8]. The output of each converter leg that comprise one phase is combined with the use of inductors, generating a single output voltage. Under ideal operation, the current would be equally shared amongst each leg of the converter, however this requirement cannot be readily satisfied unless actively controlled [2], and the finite switching frequency will result in circulating currents within the converter legs.

Furthermore, interleaved connection of converter legs generates zero-sequence circulating current (ZSCC) between the dc and ac side, increasing the semiconductor ratings and both conduction and switching losses of such topologies [9]. When the converters are operated with relatively high switching frequencies (i.e. carrier-based PWM [10] or space-vector (SVM) modulation), control of the circulating current is achieved through adjustments in the conduction times of each converter, usually through PI controllers or exact reference generation [2], [3]. A method that calculates the power reference for each of the parallel converter legs with isolated supplies without input from the other legs, applied to uninterruptible power supplies (UPS) was proposed in [5] while a discontinuous modulation scheme that allows the use of a single-core, three-limb inductor was presented in [6].

Selective harmonic elimination pulse-width modulation (SHE-PWM) offers tight control of the low-order voltage harmonics and is well-suited for high-power, low switching frequency applications [11]. However, exact elimination of harmonics is critical to the timing of transitions and deviation from the pre-calculated patterns can have an adverse effect on the accuracy of the method. Previous efforts on control of circulating currents focused on the minimisation of the ZSCC [9], [12], [13] by introducing additional transitions and eliminating low-order triplen harmonics. Such methods effectively increase the converter switching frequency [9] and limit the range where SHE-PWM solutions can be found as inclusion of triplen harmonics in the formulation transforms the problem from three-phase to single-phase [14].

The objective of this paper is to propose a controller for the circulating current of interleaved three-level converters under SHE-PWM. The task of the circulating current controller is further supported by evaluating and selecting of the SHE-PWM patterns in order to minimise the ripple of the circulating current introduced by the relatively low switching frequency of the converters.

This paper is organised as follows. Section II provides a description of the system analysing the switching states of the converter and the circulating current. Section III defines the SHE-PWM problem for interleaved multilevel converters, the effect of switching patterns on circulating currents and an evaluation of the solution for the current application. The controller for the circulating current is described in Section IV and extensive simulation results are given in Section V. Finally, the conclusions of the work are summarized in Section VI.

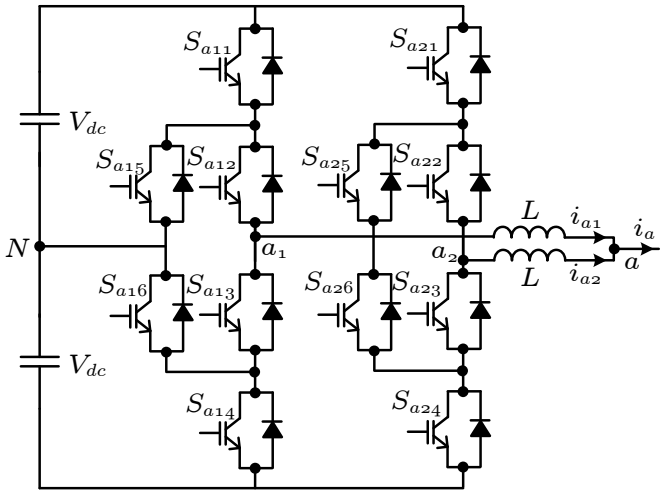

Fig. 1. One phase of the converter with two three-level active NPC converter-legs in parallel.

II. Parallel-Connected Converter Legs

A. Converter Configuration

The work in this paper focuses on two-leg interleaved converters as the one shown in Fig. 1, where two interleaved three-level active neutral-point-clamped (ANPC) converter legs form each of the phases. The main function of the inductors (L) is to limit the circulating current within the legs when the output voltage level of the two converters is different. The additional voltage levels are a result of the voltage averaging between the two outputs (V_{x1} and V_{x2}) and the phase output voltage V_x, where $x = a, b, c$ denotes the phase, is given as:

$$V_x = \frac{V_{x1} + V_{x2}}{2}. \tag{1}$$

This concept can be further extended to k three-level converters in parallel, generating $2k$+1 levels in the Thevenin output voltage given by the averaging of each converter output voltage as

$$V_x = \frac{1}{k} \sum_{j=1}^{k} V_{xj}, \tag{2}$$

and $j \in [1, \ldots, k]$ denotes each of the k interleaved converters.

The use of a single inductor per leg (Fig. 2(a)) provides a more modular and expandable system, however, practical limits in the maximum impedance [7] and the non-optimal use of magnetic material in single inductors are significant drawbacks in field applications. Coupled inductors (Fig. 2(b)) result in high differential mode impedance in the path between the interleaved converters, a concept that can be further extended to multiple interleaved converter either with one common core [4] or with multiple coupled inductors [3]. In both cases, the effect of the circulating current is a function of the differential mode impedance and, in the following analysis, coupling between the inductors has not been considered.

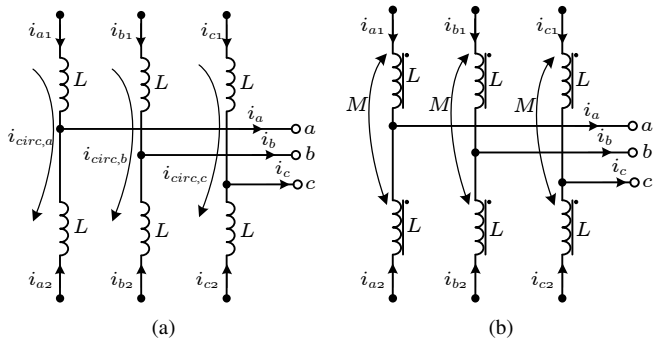

Fig. 2. (a) Single and (b) coupled inductors for interleaving of converter phase-legs.

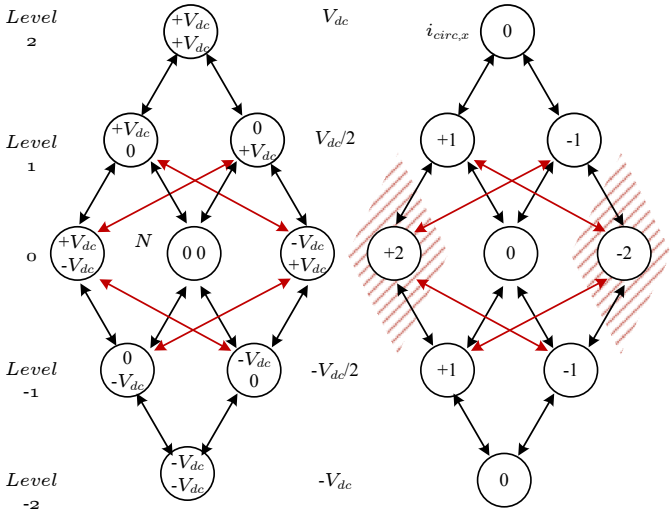

Fig. 3. Switching states of two three-level interleaved converter legs and their effect on the phase circulating current $i_{circ,x}$.

B. Converter Switching States and Circulating Current

Each state combination of the two interleaved converter legs (Fig. 3) has different effect on the circulating current ($i_{circ,x}$)

$$i_{circ,x} = \frac{i_{x1} - i_{x2}}{2} \tag{3}$$

within one phase of the converter. The differential component of the voltage is then imposed across the inductors L. This effect can be further transformed to a weighted value through normalisation with the dc-link voltage (V_{dc}) as also shown in Fig. 3.

Transitions between two different levels that involve simultaneous switching of both interleaved converters (shown in red arrows in Fig. 3) should be avoided as they lead to an unacceptable increase of the switching frequency. For the same reason, transitions between the redundant states within the same voltage level are also prohibited. The top and bottom voltage levels ($\pm V_{dc}$) are acquired with a single combination which does not affect the circulating current and, once the two zero-states that lead to excessive deviations in the circulating current (± 2) are omitted, the circulating current is affected only during the two redundant states of levels $+V_{dc}/2$ and

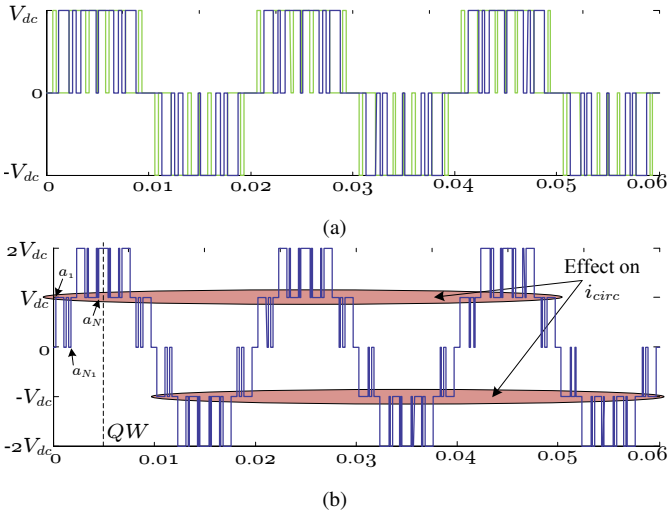

Fig. 4. Waveforms for SHE-PWM formulation (a) Two three-level waveforms and, (b) Combined optimisation based on a five-level waveform.

$-V_{dc}/2$ (Fig. 3). These redundancies will be actively used to regulate $i_{circ,x}$. During the state combinations that generate $\pm V_{dc}/2$, the voltage applied across the inductors is equal to $\pm V_{dc}$ and the rate of current change in the circulating current simply defined as

$$\frac{di_{circ,x}}{dt} = \pm \frac{V_{dc}}{2L}. \tag{4}$$

An additional component of interest in interleaved converter legs is that of the zero-sequence circulating current (ZSCC) [9], [12], [13], defined as

$$i_{ZSCC} = i_{circ,a} + i_{circ,b} + i_{circ,c}, \tag{5}$$

which , together with individual circulating currents, should be kept within limits. However, minimising the ZSCC does not necessarily lead to a minimisation of the circulating currents within each phase.

III. Selective Harmonic Elimination PWM

A. Problem Formulation and Angle Calculation

In the case of the two interleaved three-level converter legs of the previous section, the SHE-PWM problem can be formulated in two different ways, either as a combined optimisation of a five-level waveform (Fig. 4(a)) or as two separate three-level waveforms (Fig. 4(b)). When the problem is defined as a two separate three-level waveforms, the fundamental frequency component of each of the converter legs can be controlled independently, although it is preferable to share the component equally amongst the two legs. A minimisation process for the ZSCC was demonstrated in [12], however, if a formulation of the circulating current is not explicitly set within the equations, then $i_{circ,x}$ and the ZSCC cannot be accurately controlled. The SHE-PWM problem is defined as a single system of equations throughout the whole modulation index (m_a) range [11].

The five-level formulation needs to consider both the number of transitions within the quarter period (N) as well as their

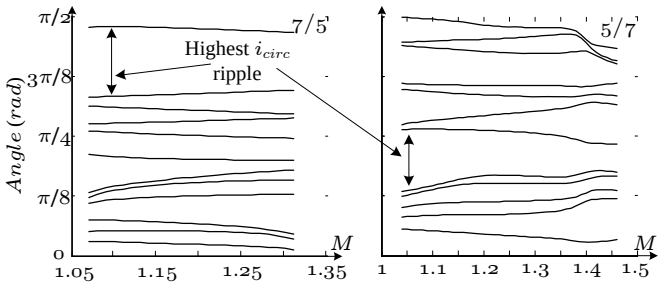

Fig. 5. SHE-PWM solution patterns for a five-level optimised waveform with 7/5 and 5/7 angle distributions.

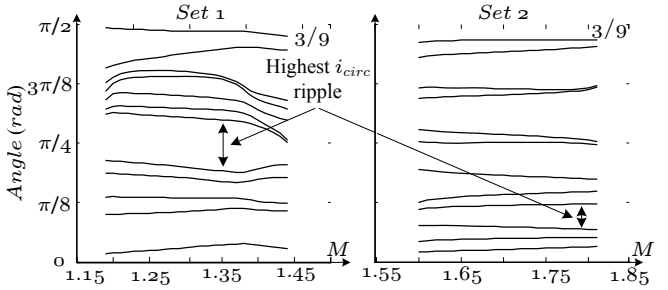

Fig. 6. SHE-PWM solution patterns for a five-level optimised waveform with 3/9 angle distribution.

distribution (N_1/N) in the different levels of the waveforms [11], as shown in Fig. Fig. 4(b) . The waveform of Fig. 4(a) shows the case of twelve ($N = 12$) switching angles per quarter period and a 5/7 distribution between the two levels of the waveform. The system of equations that describe the fundamental frequency and higher order harmonic components is:

$$\sum_{i=1}^{N_1} (-1)^{i-1} \cos(\alpha_i) + \sum_{i=N_1+1}^{N} (-1)^{i-1} \cos(\alpha_i) = m_a, \tag{6}$$

$$\sum_{i=1}^{N_1} (-1)^{i-1} \cos(n\alpha_i) + \sum_{i=N_1+1}^{N} (-1)^{i-1} \cos(n\alpha_i) = 0, \tag{7}$$

where i is the order of each switching transition, $n \in (1, 5, 7, \ldots, 3N-1)$ is the harmonic order, and N_1 the number of transitions between the zero and the first level of the waveform, which is typically considered an odd number. $m_a \in [0, 2]$ is the modulation index with the peak of the fundamental frequency component $\hat{V}_1$ defined as:

$$\hat{V_1} = \frac{4m_a}{\pi} V_{dc}. \tag{8}$$

Figs. 5 and 6 show SHE-PWM solution patterns for five-level waveforms with twelve angles per quarter-wave (QW) and different distributions of transitions among the different levels and for different m_a.

B. Evaluation and Comparison of SHE-PWM Solutions

As described in Section II-B, $i_{circ,x}$ is only affected during the $\pm V_{dc}$ voltage levels of the five level waveform. The

maximum deviation ($\Delta i_{circ,x}$) of the circulating current during a QW (and due to the imposed QW symmetry for the whole fundamental period) will be observed when state +1 is imposed for the longest time interval. This angle interval $\Delta\alpha_{\max}$ is given by

$$\Delta\alpha_{\max} = \alpha_{2g} - \alpha_{2g-1}, \tag{9}$$

where $g \in [1, N/2]$ and can be evaluated during the calculation of the solutions. Under proper control of the circulating current within each phase, the peak value of $i_{circ,x}$ will be equal to its maximum deviation which is linked to the solution pattern as:

$$\hat{i}_{circ,x} = \Delta i_{circ,x} = \frac{V_{dc}}{2L}\Delta\alpha_{\max}, \tag{10}$$

In order to minimise the peak of the circulating current, one must select SHE-PWM solutions that minimise the time interval at $\pm V_{dc}$. As SHE-PWM problems typically exhibit multiple solutions, this additional evaluation should be performed between solutions of the same or different distributions for a given m_a or range of m_a. Referring back to Fig. 5, we can observe the angles that cause the highest deviation and, subsequently, peak $i_{circ,x}$ ripple, for solution sets with 7/5 and 5/7 distribution, with the 7/5 distribution generating 25% higher peak ripple current. Similarly, SHE-PWM solutions for 3/9 distribution in two different ranges of m_a are illustrated in Fig. 6. It should be noted that Set 2 of Fig. 6 provides solutions in the overmodulation region which are typically not available when triplen harmonics are controlled.

IV. Control of the Circulating Current

This section presents the configuration of the $i_{circ,x}$ controller based on the definitions and restrictions introduced in Section III. The diagram of the proposed controller is shown in Fig. 7 and is separated into two sections, the SHE-PWM pattern generation and the selection of the switching state for the control of $i_{circ,x}$.

The first part decomposes the reference signal v_{xm} into two components, m_a and the phase angle θ. These two values could also be readily available based on the controller implementation. Based on m_a and the associated switching angles, the switching pattern is generated and made available to the second stage of the controller. The switching pattern is a normalised switching waveform similar to those of Fig. 4, and provides information related to the required output voltage level of the converter.

The second stage defines the switching states of the two converter legs based on the sign of i_{circ} and makes use of the relation between switching states and circulating current that was demonstrated in Fig. 3. The aim of the controller is to regulate the circulating current within one phase, therefore, three independent controllers are required for a three-phase system.

V. Results

Simulation studies are presented to verify the performance of the proposed controller (Fig. 7) for the two interleaved

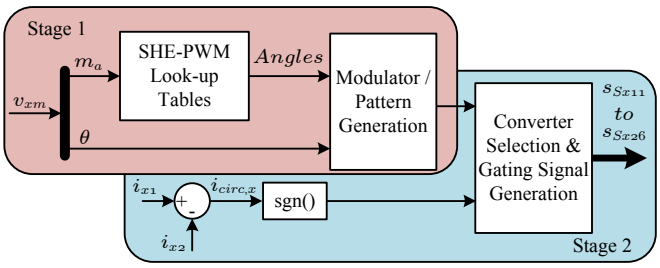

Fig. 7. Implementation of the proposed two-stage circulating current controller for two interleaved converter legs.

TABLE I
Parameters of the Simulated System

DC-Link Voltage, V_{dc}	3 kV
DC-link Capacitors, C_{dc}	3.6 mF
Arm Inductors, L	5 mH
Fundamental frequency, f_0	50 Hz
Switching Angles per QW, N	12
R_{load} & L_{load}	1Ω & 2 mH

ANPC converter legs of Fig. 1. The parameters of the system under study are given in Table I.

The results of Figs. 8 and 9 demonstrate the operation of the interleaved converters under two different SHE-PWM sets of solutions for 5/7 angle distribution and $m_a = 1.4$, which is selected at random. These results are shown in order to demonstrate the effect, the selection of a particular set of solutions can have on the circulating current of each phase and the ZSCC, with the second set demonstrating larger $\Delta\alpha_{\max}$. In both cases, the output phase currents (i_a, i_b and i_c) are identical. However, the currents through each of the interleaved converters (i_{a1} and i_{a2}) differ between the two solutions and generate significantly different circulating currents within the phases ($i_{circ,a}, i_{circ,b}$ and $i_{circ,c}$ of Fig. 2) as well as ZSCC.

The actual values are related to the selected parameters of the simulated system but the comparison of the two solution sets is generally applicable. The peak value of i_{circ} for Set 2 is 1.4 times larger than that of Set 1 while the rms value is 1.71 times larger. If the sets are compared only based on the ZSCC, the ratio of peak ZSCC values between the two solutions is just 1.13. This comparison demonstrates that the ZSCC is not the only critical component in the selection of SHE-PWM solution sets . The actual circulating currents within each phase should be generally considered as they provide a more definite metric for the stresses across the differential mode inductors in interleaved converters.

Compared to the 5/7 distribution of Figs. 8 and 9, the 3/9 distribution of Fig. 10 generates significantly lower phase circulating currents as well as ZSCC but with a higher peak in the currents within the legs (i_{a1} and i_{a2}) for the same operating point of $m_a = 1.4$. The number of switching transitions and, hence, the switching frequency of the converter in all three results is the same. Additional transitions, used to eliminate

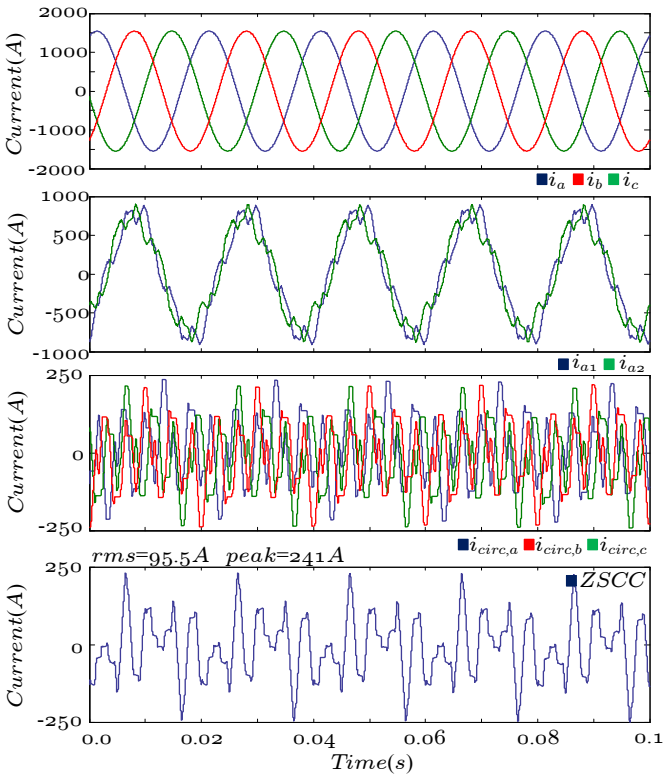

Fig. 8. Simulated phase, arm, circulating and zero sequence currents with 5/7 angle distribution and $m_a = 1.4$ (Set 1).

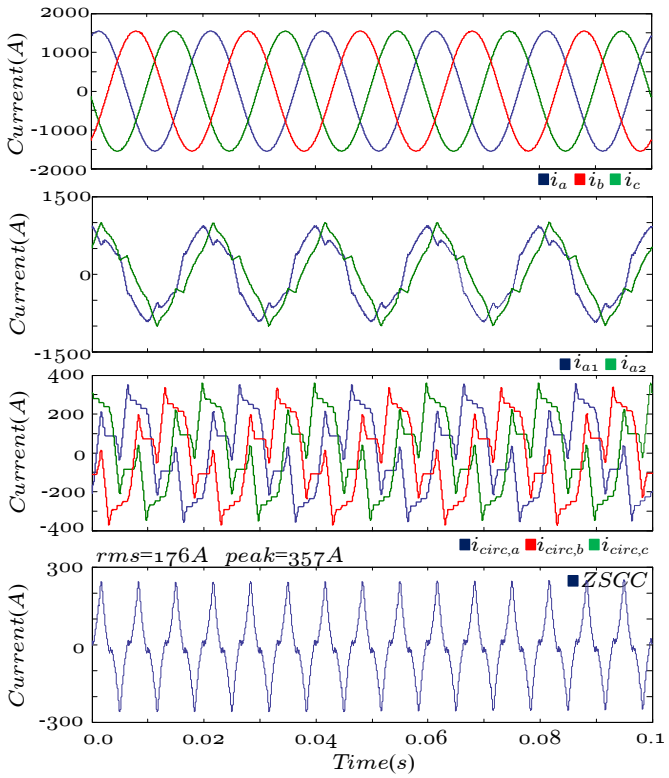

Fig. 9. Simulated phase, arm, circulating and zero sequence currents with 5/7 angle distribution and $m_a = 1.4$ (Set 2).

higher order harmonics or lower order triplen harmonics, will reduce the maximum time that the output waveform remains at a level that affects the circulating current, further reducing the peak of both $i_{circ,x}$ and ZSCC.

The proposed controller does not modify any of the switching angles in order not to affect the quality of the waveform, although such modifications may be included in order to facilitate balancing of neutral point or flying capacitor voltages. The regulation of the neutral point can also be achieved through RLC balance boosters [15] or active methods. Consequently, full utilisation of the dc-link voltage can be made and solutions well within the overmodulation range can be applied. Fig. 11 shows the output phase currents, converter currents, $i_{circ,x}$, and ZSCC for an angle distribution of 3/9 at an operating point of $m_a = 1.75$ (Fig. 6). Due to the solution pattern and the distribution of angles within the quarter-period, the converter currents (i_{a1} and i_{a2}) are well matched and both $i_{circ,x}$, and ZSCC are reduced.

To further illustrate the difference between controlling the $i_{circ,x}$ and ZSCC, the previous simulation is repeated but rather than using each phase circulating current, the ZSCC of (5) is used in the controller to determine the switching state of all three phases of the converter. The value of ZSCC (Fig. 12) is reduced compared to the previous case, when $i_{circ,x}$ is controlled. However, as there is no explicit control over the phase circulating currents, their value may reach unacceptably large values, well above the output current of each phase of the converter.

VI. Conclusion

Interleaved connection of converter legs increases the maximum power through each converter but generates circulating currents within the converter legs that should be minimised for efficient operation of the system. This becomes more challenging at low switching frequencies as unequal voltages between the interleaved converters are generally applied for longer time intervals. A circulating current controller, reducing the circulating current in each phase of two interleaved three-level ANPC converter legs under SHE-PWM, has been proposed in this paper. By selecting the switching states of the legs based on the phase circulating current $i_{circ,x}$ it is possible to limit the currents through each converter leg at a minimum, at the same time regulating the zero sequence circulating current. The proposed controller is further complemented by an evaluation and optimal selection of SHE-PWM patterns which reduce the peak of the circulating currents. Simulation results demonstrate and confirm the performance of the proposed controller.

References

[1] H. Mori, K. Matsui, K. Kondo, I. Yamamoto, M. Hasegawa, "Parallel-connected five-level PWM inverters," *IEEE Trans. Power Electron.,*, vol. 18, no. 1, Jan. 2003, pp. 173-179.

[2] J. Pou, J. Zaragoza, G. Capella, I. Gabiola, S. Ceballos, and E. Robles, "Current balancing strategy for interleaved voltage source inverters," *EPE Journal,* vol. 21, no. 1, pp. 29-34, Jun. 2011.

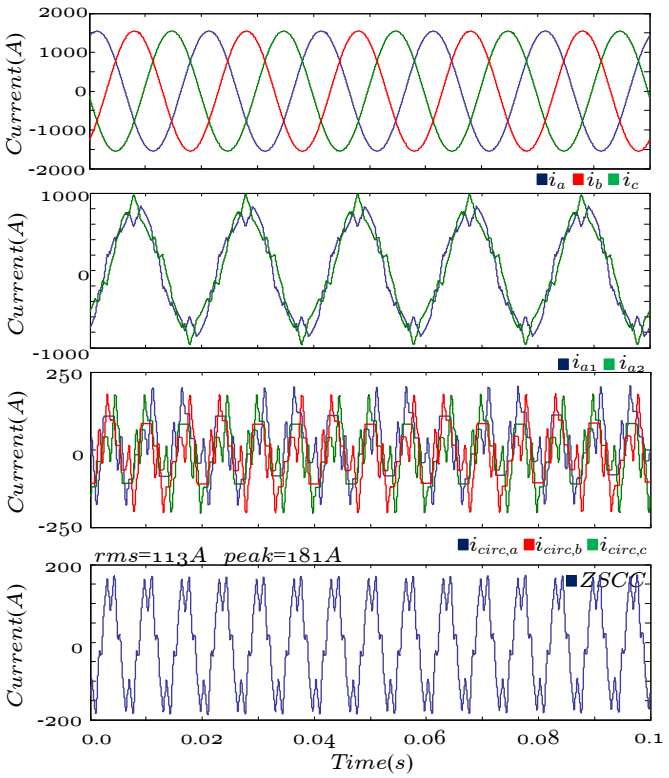

Fig. 10. Simulated phase, arm, circulating and zero sequence currents with 3/9 angle distribution and $m_a = 1.4$ (Set 1).

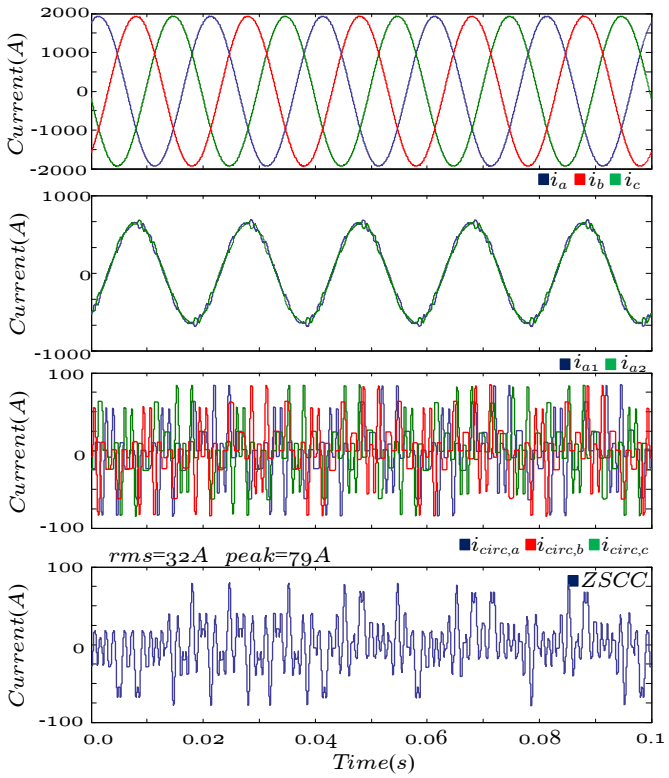

Fig. 11. Simulated phase, arm, circulating and zero sequence currents with 3/9 angle distribution and $m_a = 1.75$ (Set 1).

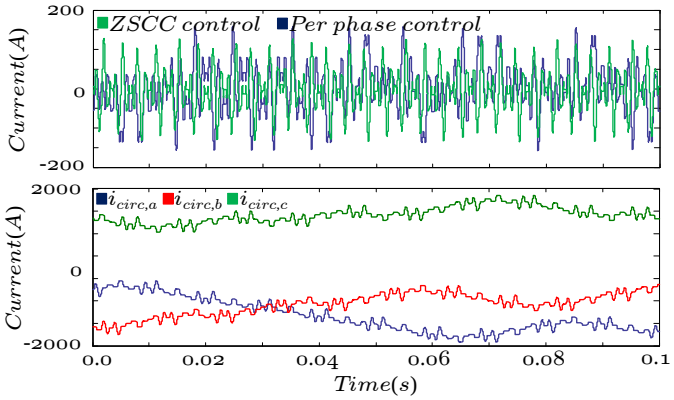

Fig. 12. Phase and zero sequence circulating currents under control of the ZSCC.

[3] G. J. Capella, J. Pou, S. Ceballos, J. Zaragoza, and V.G. Agelidis, "Current balancing technique for interleaved voltage source inverters with magnetically coupled legs connected in parallel," *IEEE Trans. Ind. Electron., early access,*, vol. 99, no. 1, pp. 1-10.

[4] G. Baoming, L. Xi, Y. Xianhao, Z. Maosong, and P. Fang Zheng, "Multiphase-leg coupling current balancer for parallel operation of multiple MW power modules," *IEEE Trans. Ind. Electr.,* vol. 61, no.3, pp. 1147-1157, Mar. 2014.

[5] T. B. Lazzarin, G. A. T. Bauer, and I. Barbi, "A control strategy for parallel operation of single-phase voltage source inverters: analysis, design and experimental results," *IEEE Trans. Ind. Electr.,* vol. 60, no. 6, pp. 2194-2204, Jun. 2013.

[6] J. Ewanchuk and J. Salmon, "Three-limb coupled inductor operation for paralleled multi-level three-phase voltage sourced inverters," *IEEE Trans. Ind. Electr.,* vol. 60, no. 5, pp. 1979-1988, May 2013.

[7] J. Shen, S. Schroder, B. Qu, Y. Zhang, K. Chen, F. Zhang, Y. Li, Y. Liu, P. Dai, and R. Zhang, "A high-performance 2x27 MVA machine test bench based on multilevel IGCT converters," in *Proc, IEEE ECCE 2014,* Sep. 2014, pp. 3224-3233.

[8] J. Pou, S. Ceballos, G. Konstantinou, G. Capella, and V.G. Agelidis, "Control strategy to balance operation of parallel connected legs of modular multilevel converters," in *Proc. of IEEE ISIE 2013,* May 2013, Taiwan, pp. 1-7.

[9] T. P. Chen, "Zero sequence circulating current reduction method for parallel HEPWM inverters between ac bus and dc bus," *IEEE Trans. Ind. Electron.,* vol. 59, no. 1, Jan. 2014, pp. 290-300.

[10] G. J. Capella, J. Pou, S. Ceballos, J. Zaragoza, G. Konstantinou, and V. G. Agelidis, "Enhanced phase-shifted PWM carrier disposition for interleaved voltage source inverters," *IEEE Trans. Power Electron., early access,*, vol. 99, no. 1, pp. 1-5.

[11] M. S. A. Dahidah, G. Konstantinou, and V. G. Agelidis, "An overview on multilevel selective harmonic elimination PWM approach: formulations, solving algorithms, implementation and applications", *IEEE Trans. Power Electron., early access,*, vol. 99, no. 1, pp. 1-16.

[12] M. Narimani and G. Moschopoulos, "Three-phase multimodule VSIs using SHE-PWM to reduce zero sequence circulating current," *IEEE Trans. Ind. Electron.,* vol. 61, no. 4, Apr. 2014, pp. 1659-1668.

[13] M. Narimani and G. Moschopoulos, "Improved method for paralleling reduced switch VSI modules: Harmonic content and circulating current," *IEEE Trans. Power Electron.,* vol. 29, no. 7, Jul. 2014, pp. 3308-3317.

[14] G. Konstantinou, V.G. Agelidis, and J. Pou, "Theoretical considerations for single-phase interleaved converters operated with SHE-PWM," *IEEE Trans. Power Electron., early access,*, vol. 29, no. 10, pp. 5124-5128.

[15] R. Stala, "A natural DC-link voltage balancing of diode-clamped inverters in parallel systems," *IEEE Trans. Ind. Electron.*, vol. 60, no.11, pp. 5008-5018, Nov. 2013.